

# Experimental determination of the strain rate dependent out-of-plane shear properties of textile-reinforced composites

W. Hufenbach, A. Langkamp, A. Hornig\*, C. Ebert

Institute of Lightweight Engineering and Polymer Technology (ILK) of the TU Dresden  
Holbeinstraße 3, 01307 Dresden, Germany

\*Andreas.Hornig@tu-dresden.de

## SUMMARY

In that paper the experimental investigation of strain rate dependent out-of-plane shear properties of glass fibre textile-reinforced composites with thermoplastic polypropylene matrices is discussed. The focus of the investigations is set on the out-of-plane shear laminate properties determined with servohydraulic high speed testing unit and lightweight-IOSIPESCU-device.

*Keywords:* strain rate dependency, out-of-plane properties, glass fibre reinforced composites, thermoplastic matrices, crash and impact loads

## INTRODUCTION

Advanced specific mechanical properties and a high energy absorption capacity qualify textile-reinforced composites for the design of material and energy efficient lightweight structures e.g. in vehicle industries and mechanical engineering, where structures are subjected to crash and impact loads [1]. For a reliable structural design of security-relevant, highly dynamically loaded lightweight structures [2], the knowledge of the strain rate dependent material behaviour with statistically confirmed material properties and validated material models as well as appropriate simulation methods have to be provided. Especially for complex loading conditions the design process requires the application of the Finite Element Method. The implemented material models which consider the strain rate dependent anisotropic damage and failure behaviour [3] require an extensive set of characteristic material data. In recent investigations advanced methods for the highly dynamical material characterisation have been elaborated and the strain rate dependent in-plane properties of textile-reinforced composites have been determined [4,5]. Besides that, the consideration of the strain rate dependency of the out-of-plane laminate properties is essential in the design process in order to evaluate complex 3D states of stress. A reliable experimental characterisation method is still to be defined for this.

The proposed method for the investigations of the out-of-plane material behaviour is to use a servo hydraulic high speed testing unit INSTRON VHS 160/20 for strain rates from  $\dot{\epsilon} = 6 \times 10^{-3} \text{ s}^{-1}$  up to  $6 \times 10^1 \text{ s}^{-1}$  in combination with a lightweight IOSIPESCU testing device. The focus of the experimental investigations here are set on two types of composites made of a conventional twill fabric with commingled hybrid glass-polypropylene rovings (Twintex<sup>®</sup>) and a 3D reinforced multilayered flat bed weft knitted fabric of hybrid glass fibre-polypropylene yarn (GF-PP-MKF) respectively [6].

A special process technology has been developed to manufacture 100 mm thick specimens.

## INVESTIGATED MATERIAL CONFIGURATIONS

### Textile Architecture

For the studies two types of layered composites have been used. Both composite configurations are based on glass fibre reinforcements with different textile architectures and a thermoplastic polypropylene matrix.

On the one hand a 3D reinforced textile architecture was used (Figure 1). The multi-layered weft knitted fabric (MKF) has been developed and fabricated by the Institute of Textile and Clothing Technology at the TU Dresden [7,8]. A commingled Twintex<sup>®</sup> hybrid E-glass - polypropylene yarn has been used. The preform lay-up corresponds to eight symmetrically arranged layers ( $[90/0//0/90]_4$ ), resulting in a fibre volume fraction of 47 %.

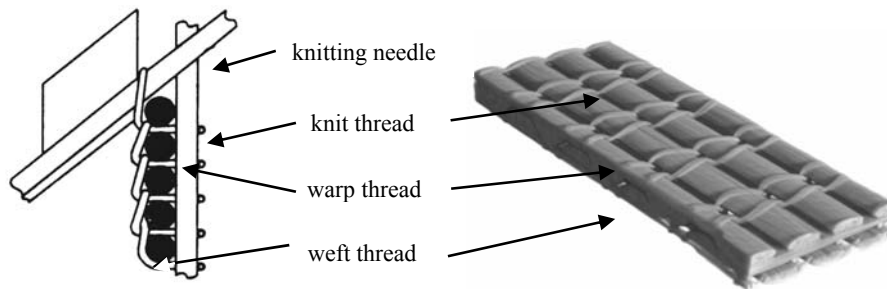


Figure 1: MKF, left: basic architecture (schematic) [7], right: two symmetrically arranged layers (CT-scan) [9]

On the other hand composites made of the commercially available woven fabric Twintex<sup>®</sup> have been investigated. The balanced twill 2/2 consists of commingled hybrid glass-polypropylene rovings, resulting in a fibre volume fraction of 35 % after consolidation.

### Manufacture and Specimen Configuration

The consolidation of both material setups (MKF, Twintex<sup>®</sup>) is done by stacking the textile preforms, heating above the melting temperature of the polypropylene matrix (180 °C – 230 °C) and applying a moderate pressure in an autoclave. For configuration 1 and 2 this was done with the support of a vacuum bag. For configuration 3 an additional process step has been developed (Figure 2b) to ensure a more advantageous temperature profile during heating and consolidation cycle. A pre-consolidated laminate is cut into strips, which are stacked in the developed tool. In an additional autoclave consolidation cycle a 100 mm thick composite block (Figure 2c) is produced which can be used for specimen manufacture. The specimens have finally been notched in a grinding process.

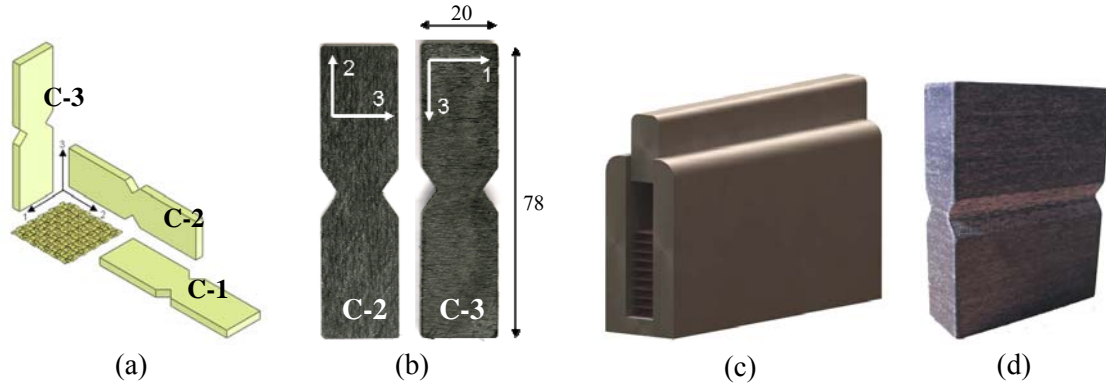


Figure 2: (a) Schematic test configurations: C-1, C-2, C-3 and their orientations  
 (b) Exemplary specimens and geometry (45° V-notch)  
 (c) Consolidation tool for configuration C-3 specimen manufacturing  
 (d) Consolidated and machined configuration C-3 specimen block (uncut)

According to figure 2a three specimen configurations have been tested with different material setups, all consisting of stacked bi-directional textile-reinforced single plies with equal properties in both directions. A detailed overview of the testing program is given in Table 1.

Table 1: Specification of the tested configurations and material setups

con-figuration	plane of shear stresses	material		tested specimen per material	strain rates [s <sup>-1</sup> ]	ascertainable properties
		MKF	Twintex <sup>®</sup>			
C-1	12	x	x	54	0,006-60	R <sub>12</sub> , G <sub>12</sub>
C-2	23	x	x	36	0,006-60	R <sub>23</sub> , G <sub>23</sub>
C-3	31		x	18	0,04-40	R <sub>31</sub> , G <sub>31</sub> ,

Based on continuum mechanics shear stresses are seen as attributive, thus  $\tau_{12} - \tau_{21}$ ,  $\tau_{13} - \tau_{31}$  and  $\tau_{23} - \tau_{32}$  with the corresponding engineering shear stiffnesses  $G_{12}$ ,  $G_{13}$  and  $G_{23}$ . Based on the 50/50 bidirectional textile architecture of the composite configurations investigated here, the shear stiffness and strength in 23- and 31-direction (C-2 and C-3) ought to be equal ( $G_{23} = G_{31}$ ,  $R_{23} = R_{31}$ ).

## EXPERIMENTAL PROCEDURE

For the investigations and the characterisation of materials at high loading speeds a servohydraulic high velocity test system (SHP) INSTRON VHS 160/20 has been used. Special adaptations of the test equipment allow highly-dynamic tensile, compression and shear tests. The SHP enables tests of materials and components at high deformation speeds of up to 20 m/s and a maximum force of 160 kN.

In addition to that, a new type of lightweight IOSIPESCU device (Fig. 3, right) was developed for highly-dynamic shear tests, which in comparison to a conventional IOSIPESCU device offers a weight reduction of approx. 80 % and reduces the influence of inertia effects significantly.



Figure 3 Lightweight test devices for tensile (left) and shear (right) tests

Aside from machine-integrated measuring equipment for recording the machine path, the force and effective acceleration, a laser-DOPPLER-extensometer for the local measurement of strain as well as high-speed cameras are used for the analysis of the deformation and failure behaviour. The laser-DOPPLER-extensometer employs the function principle of laser-optical speed measurement by means of a difference-DOPPLER-method on two stationary observation points and allows the contact-less measurement of strain at speeds of up to 30 m/s.

High-speed camera systems were used for the visual analysis of the damage and failure processes taking place within milliseconds. For this purpose, the ILK uses high-speed video cameras with maximum frame rates of up to 200,000 images per second.

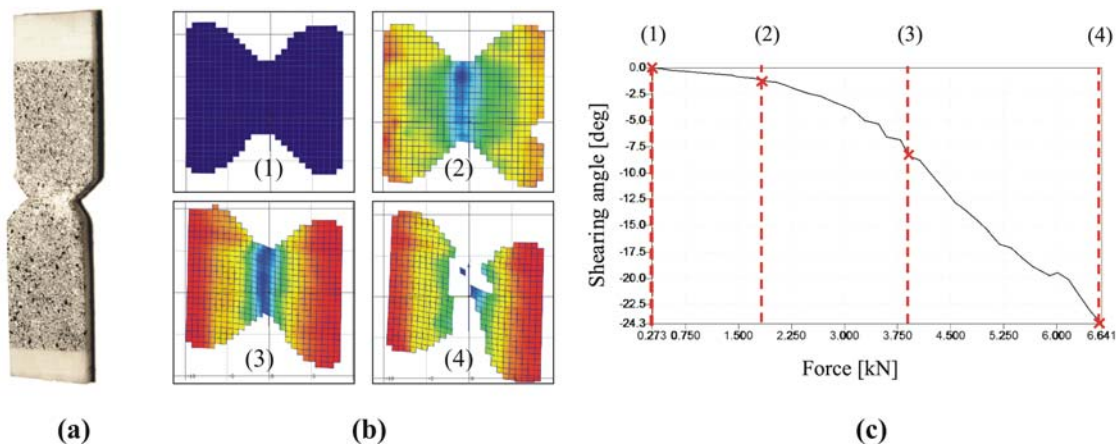


Figure 4: (a) Exemplary IOSIPESCU-specimen with stochastic pattern (Twintex<sup>®</sup>, C1, deformed)

(b) Four states of full field high speed shear deformation analysis (1-unloaded, 2-elastic shear deformation, 3-plastic shear deformation, 4-fragmentation)

(c) Shearing angle vs. force diagram with related deformation states

The high-speed camera systems can also be used to gain information on dislocation and distortion fields and have been used in combination with ARAMIS, an optical 3D deformation measurement system, so that the online measurement and analysis of the

deformation and strain field during highly dynamic loading was enabled. As an example in figure 4 an IOSIPESCU-shear specimen with stochastic pattern (a), four states of full field high speed shear deformation analysis (b) and a shear angle vs. force diagram are shown exemplarily.

## RESULTS AND DISCUSSION

### Shear in 12-plane (C-1)

A detailed examination of the stress-strain behaviour, the damage process and strain rate dependent properties can be found in the following chapter for C-1 test configuration. In figure 5 the stress-strain-behaviour for both material configurations (MKF, Twintex<sup>®</sup>) at  $\dot{\varepsilon} \approx 7 \text{ s}^{-1}$  are displayed. The identification of the initial failure and stiffness has been done by using the 5 % strain limit, according to the German standard DIN EN ISO 14129 for the determination of the in-plane shear modulus and shear strength. The author emphasizes, that this value is not a phenomenological based limit, but remains constant, independently of the material configuration or strain rate.

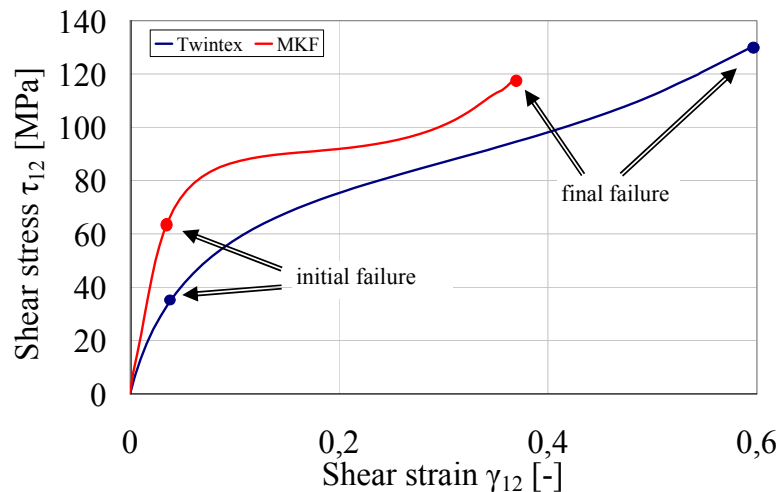


Figure 5: C-1 characteristic stress-strain plots for Twintex<sup>®</sup> and MKF at  $\dot{\varepsilon} = 7,5 \text{ s}^{-1}$  and  $6 \text{ s}^{-1}$  respectively indicating varying deformation and failure behaviour

The mechanical behaviour for both materials shows a linear and non-linear domain. The initial failure indicates the beginning of material non-linear behaviour and can be seen as the onset of damage evolution. MKF composites generally show an advanced initial failure level and stiffness response, but the final failure occurs at significantly lower strains and strengths. That trend is independent of the strain rate (figure 5). The reason can be found in the textile architecture of MKF. Its craned warp and weft fibres cause a “delayed” onset of damage, while the rovings of Twintex<sup>®</sup>-composites have a phase of crimp reduction.

The effect of the different strain rate regimes can be seen in figure 6. The trend of a rising strength and stiffness with rising strain rate occur in both material configurations. The occurring damage mechanisms and the resulting curve characteristics caused by the textile architecture remain unchanged throughout the investigated strain rates. In this

respect, Twintex<sup>®</sup> behaves more compliant but with a higher ultimate strength than MKF. Since the material shear behaviour in the 12-plane is considered to be matrix dominated, it is assumed that the strain rate dependency is mainly caused by the polypropylene.

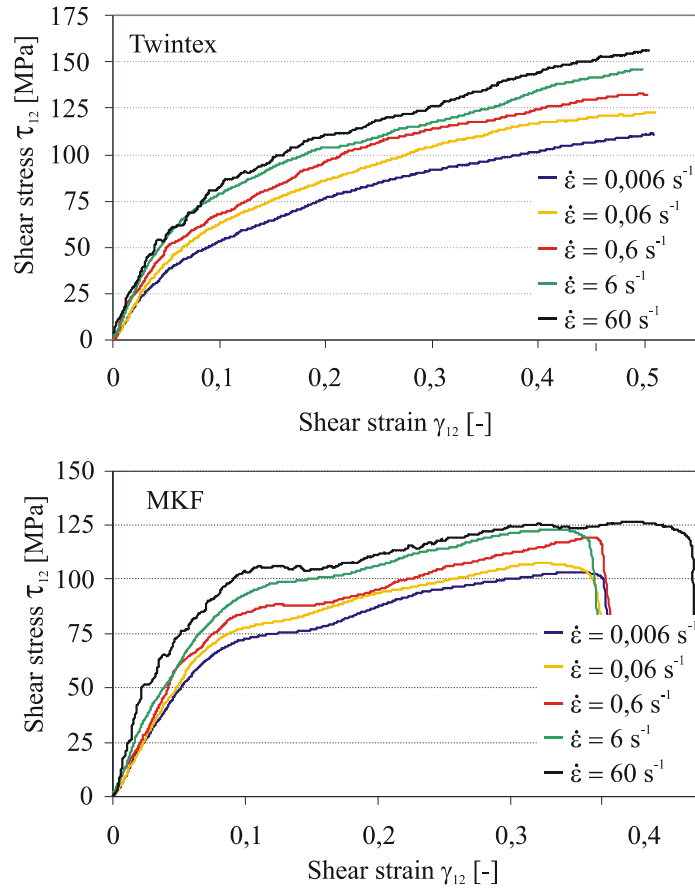


Figure 6: Stress-strain curves of test configuration C-1 at different strain rates of Twintex<sup>®</sup> (top) and MKF composites (bottom)

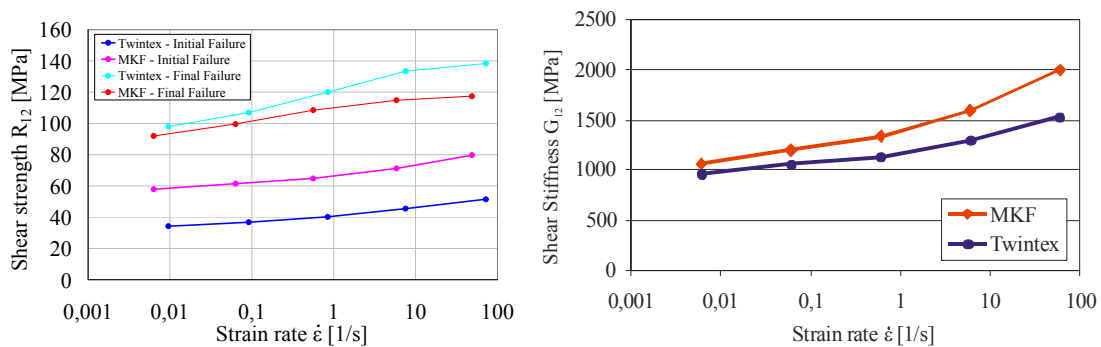


Figure 7: Strain rate dependent shear strengths  $R_{12}$  and stiffness  $G_{12}$  of Twintex<sup>®</sup> and MKF composites

Both materials show a comparable strain rate dependency (figure 7) with regard to both strength and stiffness. Particularly, with an increasing strain rate of five orders of magnitude, the initial failure strengths raises app. by 75 % for Twintex<sup>®</sup> and MKF

composites and the stiffness by 120 % (Twintex<sup>®</sup>) and 95 % (MKF) respectively. The final failure diverges with rising strain rates, indicating that the difference between crimped and non-crimped fibres and the influence of the matrix respectively gains relevance at higher rates, causing a jump in the final failure strengths of 55 % for Twintex<sup>®</sup> and 30 % for MKF.

### Shear in 23-plane (C-2)

The stress-strain-curves of MKF and Twintex<sup>®</sup> composites displayed in figure 8 for shear loading in the 23-plane show no significant influence of the strain rate on the deformation and failure behavior.

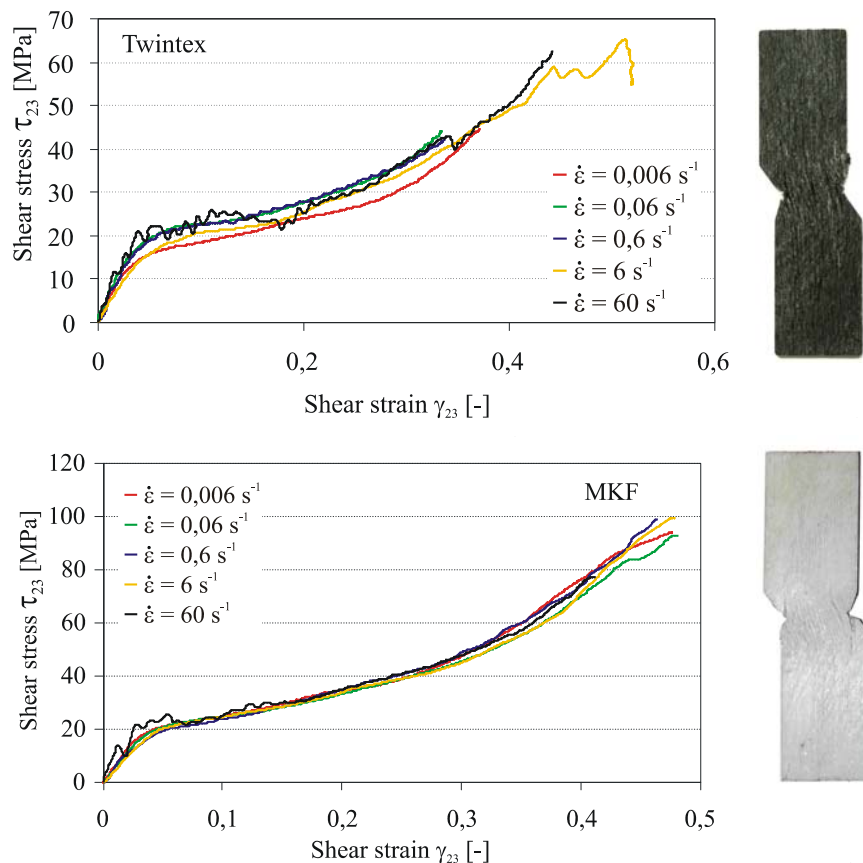


Figure 8: Stress-strain curves of specimen configuration C-2 at different strain rates of Twintex<sup>®</sup> (top) and MKF (bottom)

As shown in figure 8 the initial and final failure level of both material configurations is rate independent, exhibiting the same characteristic behaviour throughout the whole tested strain rate span. The initial failure mode caused by pure  $\tau_{23}$ -shear and is an interlaminar mode. The failure strength is on the same level for both material configurations, indicating equal interlaminar shear strengths of both materials. This type of failure is strongly influenced by the fibre-size-matrix configuration and thus it appears that it can be treated as independent of the textile architecture. The fracture pattern of the initial failure indicates a dominating interface failure, which appears to be strain rate independent.

### Shear in 31-plane (C-3)

The IOSIPESCU-experiments in the 31-plane have been performed for Twintex<sup>®</sup> only. The occurring interlaminar failure appears to be strain rate independent (figure 9). The failure strength and strain level is equal to the initial failure event of C-2 (figure 8 bottom).

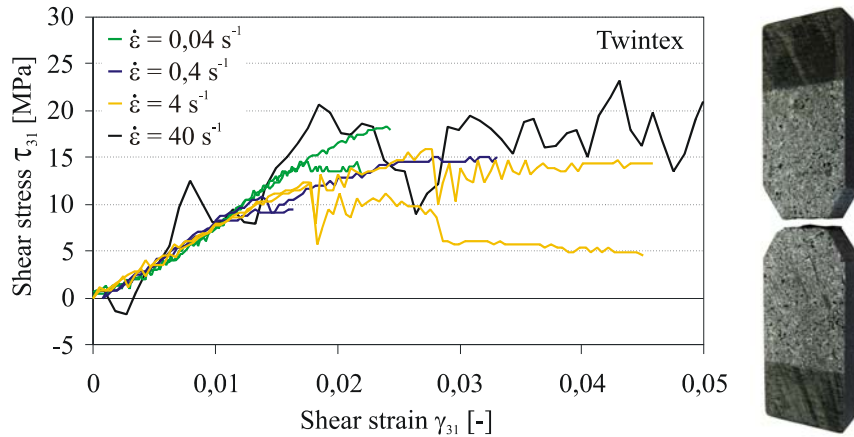


Figure 9: Stress-strain curves of specimen configuration C-3 at different strain rates of Twintex<sup>®</sup>

The measurement accuracy is not comparable to the previous experiments due to the low failure stress and strain levels. Statistically firm results are to be proven in order to reduce the present uncertainty and scatter.

### CONCLUSIONS

The presented work deals with the determination of the shear deformation and failure behaviour different of textile-reinforced composites under consideration of strain rate effects. For the experimental characterisation of the shear properties a lightweight IOSIPESCU test device within a servohydraulic high velocity test system has been used. The additional use of a high speed camera system with the optical full field measurement system ARAMIS enables the localised analysis of the shear strains in the area of interest, instead of interpreting the global response.

The determination of strain rate dependent properties is highly relevant as a basis for the structural evaluation of components under elevated loading-velocities. The strain rate influence on the strength and stiffness is considerably reduced for the out-of-plane properties (figures 8 and 9) and can be treated as negligible in contrast to the in-plane-shear properties (figure 7), which are considered to be highly significant. Vital for potential constitutive models for the investigated materials is the consideration of a directional strain rate dependency.

The shear behaviour in the 12-plane can be divided in a linear domain up to an initial failure threshold followed by a highly non-linear damage progression. A coupled failure mechanism has been identified in the 23-plane, where initially pure interlaminar shear failure occurs, followed by a secondary mixed mode.



## ACKNOWLEDGEMENTS

The authors wish to express their thanks to the Deutsche Forschungsgemeinschaft (DFG) for their financial support within the scope of Collaborative Research Centre (SFB) 639, subproject C4.

## References

1. Hufenbach, W. (Ed.): Textile Verbundbauweisen und Fertigungstechnologien für Leichtbaustrukturen des Maschinen- und Fahrzeugbaus. 2007, Progress media-Verlag, Dresden
2. Hufenbach, W.; Gude, M.; Ebert, Chr.: Tailored 3D-textile reinforced composites with load-adapted property profiles for crash and impact applications. *Composites*, 6 (2006) 3, 8-13
3. Hufenbach, W.; Gude, M.; Hornig, A.; Böhm, R.; Zschoyge, M.: Numerical and experimental deformation and failure analysis of 3D-textile reinforced lightweight structures under impact loads. ECCM 13, June 2-5 2008, Stockholm, Sweden
4. Gude, M.; Hufenbach, W.; Ebert, Ch.: Characterization and simulation of the strain rate dependent material behaviour of novel 3D-textile reinforced composites. ECCM 13, June 2-5 2008, Stockholm, Sweden
5. Song, B.; Weinong, Ch.: Quasi-static and dynamic compressive behaviors of S-2 glass/SC15 composite. *Composite Materials*, 37 (2003) 19, 1723-1743
6. Diestel, O.; Offermann, P.: Thermoplastische GF/PP-Verbunde aus biaxial verstärkten Mehrlagengestricken – Werkstoff zur Verbesserung der passiven Fahrzeugsicherheit? *Technische Textilien / Technical Textiles* 43 (2000) 4, 274-277
7. Cherif, C.; Diestel, O.; Gries, T.: Textile Verstärkungen, Halbzeuge und deren textiltechnische Fertigung. Hufenbach, W (Ed.): Textile Verbundbauweisen und Fertigungstechnologien für Leichtbaustrukturen des Maschinen- und Fahrzeugbaus. 2007, Progress media-Verlag, Dresden
8. Cebulla, H.; Diestel, O.; Offermann, P.: “Polar Orthotropic Reinforced Weft Knitted High Performance Sphere and Helmet”, 34. Int. SAMPE Tech. Conf., Baltimore (USA), 2002, S. 39-24
9. Hufenbach, W.; Petrinic, N.; Hornig, A.; Langkamp, A.; Gude, M.; Wiegand, J.: Delamination behaviour of 3D-textile reinforced composites – Experimental and numerical approaches. *The e-Journal of Nondestructive Testing*, 1st Conference on damage in composite materials, Stuttgart, 18.-19.September 2006 11 (2006), Nr. 12